



## Ordering Mechanisms in Confined Diblock Copolymers

YOAV TSORI

*ESPCI, 10 Rue Vauquelin, Paris 75231, Cedex 05, France*

DAVID ANDELMAN

*School of Physics and Astronomy, Raymond and Beverly Sackler Faculty of Exact Sciences,  
Tel Aviv University, Ramat Aviv, Tel Aviv 69978, Israel*

andelman@post.tau.ac.il

**Abstract.** We present several ordering mechanisms in diblock copolymers. For temperatures above the order-disorder temperature and in the weak segregation regime, a linear response theory is presented which gives the polymer density in the vicinity of confining flat surfaces. The surfaces are chemically patterned where different regions attract different parts of the copolymer chain. The surface pattern or template is decomposed into its Fourier modes, and the decay of these modes is analyzed. The propagation of the surface pattern into the disordered bulk is given for several types of patterns (e.g. uniform and striped surface). It is further shown that complex morphology can be induced in a thin film even though the bulk is disordered. We next consider lamellar diblock copolymers (low temperature regime) in the presence of a striped surface. It is shown that lamellae acquire a tilt with respect to the surface, if the surface periodicity is larger than the bulk one. The lamellae close to the surface are strongly distorted from their perfect shape. When the surface and lamellar periodicities are equal, the lamellae are perpendicular to the surface. Lastly, the transition from parallel to perpendicular lamellae in a thin film is presented. The transition between the two states depends on the surface separation and strength of surface interactions. We further calculate the phase diagram in the presence of perpendicular electric field favoring perpendicular ordering. In the strong segregation limit we introduce a simple model to calculate the phase diagram of the fully parallel, fully perpendicular and mixed (parallel and perpendicular) states.

**Keywords:** block copolymers, lamellar ordering, electric fields

### 1. Introduction

Block copolymers (BCP) are polymeric systems where each polymer chain is composed of several chemically distinct homopolymer blocks, connected together by a covalent bond. At high temperatures, BCP have a disordered phase, while at low temperatures, the macroscopic phase separation is hindered because the two (or more) immiscible sub-chains cannot be detached from each other as they try to phase separate. Hence, BCP phase separate into a variety of micro-ordered structures, with characteristic size which depends on the BCP chain length and other system parameters [1]. The morphology and structure of the prevailing phase

depends on the lengths of constituent sub-chains (also called blocks), the chemical interactions between the blocks, the temperature and the chain architecture. The BCP micro-domain size ranges from about 10 to several hundreds nanometers. This fundamental periodicity should be distinguished from the macro-domain size of several micrometers where one ordered phase (e.g., a lamellar phase) breaks into many domains (or grains) each having a different orientation and separated by grain boundaries.

Block copolymers can be viewed as composite materials from the mechanical point of view [2]. By connecting together a stiff (rod-like) block with a flexible (coil) block, one can obtain a material which is rigid, but not

brittle [3]. Moreover, the interplay between flexibility and toughness can be controlled by temperature. Different chain architecture (ring or star-like) may lead to novel mechanical and flow properties [4]. In addition, BCPs have many industrial uses because the length scales involved are smaller or comparable to the wavelength of light. These applications include waveguides, photonic band gap materials and other optoelectronic devices [5] and dielectric mirrors [6].

Recent studies have highlighted the role of an applied electric field in creating well aligned BCP structures. An electric field has been applied to a polymer film confined by one smooth and one topographically-patterned electrodes. The field creates an instability in the polymer film which replicates the pattern on the electrode [7]. In BCPs, electric field is effective in aligning micro-domains in a desired direction, as has been shown theoretically [8–10] and experimentally [11, 12]. In a thin film, for example, further removal of one polymer component can facilitate the creation of anti-reflection coatings for optical surfaces [13] or a surface with highly ordered features. Lastly, cylindrical domains of polystyrene (PS)/polymethylmethacrylate (PMMA) diblock copolymer have been used by Russell, Steiner, Thurn-Albrecht and co-workers as a basis to an array of long and aligned conducting domains (nano-wires) with typical size in the range of 100 nm [14].

The present paper deals with several mechanisms that can be used to achieve a desired ordering in a BCP melt. We consider in Section 2 thin films of A/B BCPs between two flat, parallel surfaces. In the disordered phase we give a description of the polymer density as a function of a pre-designed and fixed chemical pattern on the surface. The decay of surface  $q$ -modes into the bulk is analyzed on the level of a linear-response theory. The influence of confining surfaces on lamellar BCPs is studied in Section 3. We find that for a one dimensional striped surface pattern (composed of regions of alternating A and B preference) the lamellae are tilted with respect to the parallel surfaces. In this tilted state the lamellae adjust their periodicity to the surface one, leading to a better surface coverage. If the surface and lamellar periodicities are equal, the lamellae are formed perpendicular to the surfaces. Alignment of confined lamellae by external electric fields is studied in Section 4. It is shown that because different polymers have different values of the dielectric constant, the electrostatic energy favors an orientation of lamellae in a direction perpendicular to the confining electrodes.

This electrostatic tendency can be used to overcome interfacial interactions with the bounding electrodes and align structures in a desired direction.

## 2. Confined di-BCP in the Disordered Phase

Let us consider first an A/B di-BCP melt in the high temperature and disordered state, above the Order-Disorder Temperature (ODT) defined below. The BCP is confined by one or two flat, chemically patterned surfaces. Although the bulk BCP is disordered above the ODT, there is an oscillatory decay of the A/B block correlations and resulting ordering induced by the surface is rather complex. In the vicinity of the ODT this ordering can become long range leading to a strong effect. With the definition of the order parameter  $\phi(\mathbf{r}) \equiv \phi_A(\mathbf{r}) - f$  as the local deviation of the A monomer concentration from its average, the bulk free energy can be written as:

$$\frac{Nb^3 F_b}{k_B T} = \int \left\{ \frac{1}{2} \tau \phi^2 + \frac{1}{2} h (\nabla^2 \phi + q_0^2 \phi)^2 + \frac{1}{6} \Lambda \phi^3 + \frac{u}{24} \phi^4 \right\} d^3 r \quad (1)$$

$d_0 = 2\pi/q_0$  is the fundamental periodicity in the system, and is expressed by the polymer radius of gyration  $R_g$  through  $q_0 \simeq 1.95/R_g$ . The parameter  $\tau = 2\rho N(\chi_c - \chi)$  measures the distance from the critical point ( $\tau = 0$ ) in terms of the Flory parameter  $\chi \sim 1/T$ . At the critical point (or equivalently the ODT)  $\chi_c \simeq 10.49/N$ . In addition,  $b$  is the Kuhn statistical segment length,  $h = 1.5 \rho c^2 R_g^2 / q_0^2$  and  $\rho = 1/Nb^3$  is the chain density per unit volume.  $\Lambda$  and  $u$  are the three- and four-point vertex functions calculated by Leibler [15]. Below we restrict ourselves to lamellar phases of symmetric BCPs ( $f = \frac{1}{2}$ ,  $\Lambda = 0$ ), and set for convenience  $c = u/\rho = 1$  throughout the paper.

BCPs [16–18] and other systems with spatially modulated phases [19, 20] have been successfully described by Eq. (1) or similar forms of free energy functionals. The free energy, Eq. (1), describes a system in the disordered phase having a uniform  $\phi = 0$  for  $\chi < \chi_c$  (positive  $\tau$ ), while for  $\chi > \chi_c$  (negative  $\tau$ ), the system is in the lamellar phase for  $f = \frac{1}{2}$ ,  $\Lambda = 0$ , and can be described approximately by a single  $q$ -mode  $\phi = \phi_L \exp(i\mathbf{q}_0 \cdot \mathbf{r})$ . The amplitude of the sinusoidal modulations is given by  $\phi_L^2 = -8\tau/u$ . The validity of Eq. (1) is limited to a region of the phase diagram

close enough to the critical point where the expansion in powers of  $\phi$  and its derivatives is valid, but not too close to it, because then critical fluctuations become important [21, 22]. This limit employed hereafter is called the weak segregation limit.

The presence of chemically heterogeneous surfaces is modeled by adding short-range surface interactions to the free energy,

$$F_s = \int [\sigma(\mathbf{r}_s)\phi(\mathbf{r}_s) + \tau_s\phi^2(\mathbf{r}_s)] d^2\mathbf{r}_s \quad (2)$$

The integration is carried out over the position of the confining surfaces parameterized by the vector  $\mathbf{r}_s$ . The surface field  $\sigma(\mathbf{r}_s)$  has an arbitrary but fixed spatial variation and is coupled linearly to the BCP surface concentration  $\phi(\mathbf{r}_s)$ . Preferential adsorption of the A block ( $\phi > 0$ ) onto the *entire* surface is modeled by a constant  $\sigma < 0$  surface field, resulting in parallel-oriented layers (a perpendicular orientation of the chains). One way of producing such a surface field in experiments is to coat the substrate with random copolymers [23, 24]. If the pattern is spatially modulated,  $\sigma(\mathbf{r}_s) \neq 0$ , then the A and B blocks are attracted to different regions of the surface. The coefficient of the  $\phi^2$  term in Eq. (2) is taken to be a constant surface correction to the Flory parameter  $\chi$  [25, 26]. A positive  $\tau_s$  coefficient corresponds to a suppression of surface segregation of the A and B monomers.

For simplicity we consider first BCP confined by one surface located at  $y = 0$  as is depicted in Fig. 1(a). A generalization to two parallel surfaces is straightforward and will be given later. The surface chemical pattern  $\sigma(\mathbf{r}_s) = \sigma(x, z)$  can be decomposed in terms of its  $q$ -modes

$$\sigma(x, z) = \sum_{\mathbf{q}} \sigma_{\mathbf{q}} e^{i(q_x x + q_z z)} \quad (3)$$

where  $\mathbf{q} = (q_x, q_z)$ , and  $\sigma_{\mathbf{q}}$  is the mode amplitude. Similarly,  $\phi$  can be written as a sum

$$\phi(\mathbf{r}) = \sum_{\mathbf{q}} \phi_{\mathbf{q}}(y) e^{i(q_x x + q_z z)} \quad (4)$$

Close to the ODT the free energy is stable to second order in  $\phi$ , and higher order terms (i.e. the  $\phi^4$  term) can be neglected. Then  $\phi(\mathbf{r})$  is inserted into Eq. (1) and an integration over the  $x$  and  $z$  coordinates is carried out. Minimization with respect to  $\phi_{\mathbf{q}}(y)$  yields the Euler-Lagrange equation

$$[\tau/h + (q^2 - q_0^2)^2] \phi_{\mathbf{q}} + 2(q_0^2 - q^2) \phi_{\mathbf{q}}'' + \phi_{\mathbf{q}}'''' = 0 \quad (5)$$

Note that the equation is linear and that the Fourier harmonics  $\phi_{\mathbf{q}}$  are not coupled. The boundary conditions are rather complicated because they couple the value of the amplitude and its derivatives at the surface. They result from minimization of the full free energy expression, Eqs. (1) and (2)

$$\phi_{\mathbf{q}}''(0) + (q_0^2 - q^2) \phi_{\mathbf{q}}(0) = 0 \quad (6)$$

$$\sigma_{\mathbf{q}}/h + 2\tau_s \phi_{\mathbf{q}}(0)/h + (q_0^2 - q^2) \phi_{\mathbf{q}}'(0) + \phi_{\mathbf{q}}'''(0) = 0 \quad (7)$$

Since Eq. (5) is linear, its solution is a sum of exponentials,

$$\phi_{\mathbf{q}}(y) = A_{\mathbf{q}} \exp(-k_{\mathbf{q}} y) + B_{\mathbf{q}} \exp(-k_{\mathbf{q}}^* y) \quad (8)$$

where the modulation constant  $k_{\mathbf{q}}$  and the amplitude  $A_{\mathbf{q}}$  are given by

$$\begin{aligned} k_{\mathbf{q}}^2 &= q^2 - q_0^2 + i\sqrt{\tau/h} \\ A_{\mathbf{q}} &= -\sigma_{\mathbf{q}}(4\tau_s + 2\text{Im}(k_{\mathbf{q}})\sqrt{\tau h})^{-1} \end{aligned} \quad (9)$$

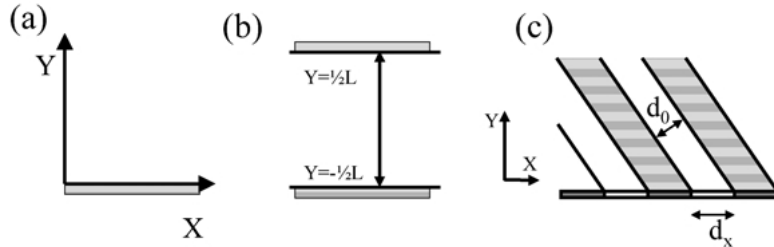


Figure 1. Schematic illustration of the coordinate system for BCP confined by one (part (a)) or two (part (b)) planar and parallel surfaces. (c) Lamellae are formed tilted with respect to the surface if the surface periodicity  $d_x$  is larger than the natural one  $d_0$ .

In the above  $\text{Re}(k_q) > 0$  ensuring that  $\phi_q \rightarrow 0$  as  $y \rightarrow \infty$ . This restricts the solution  $\phi_q$  to be a sum of only two (out of four) exponential terms.

The two lengths,  $\xi_q = 1/\text{Re}(k_q)$  and  $\lambda_q = 1/\text{Im}(k_q)$ , correspond to the exponential decay and oscillation lengths of the  $q$ -modes, respectively. For fixed  $\chi$ ,  $\xi_q$  decreases and  $\lambda_q$  increases with increasing  $q$ . Close to the ODT and for  $q > q_0$  we find finite  $\xi_q$  and  $\lambda_q \sim (\chi_c - \chi)^{-1/2}$ . However, all  $q$ -modes in the band  $0 < q < q_0$  are equally “active”, i.e., these modes decay to zero very slowly in the vicinity of the ODT as  $y \rightarrow \infty$ :  $\xi_q \sim (\chi_c - \chi)^{-1/2}$  and  $\lambda_q$  is finite. Therefore, the propagation of the surface imprint (pattern) of  $q$ -modes with  $q < q_0$  into the bulk can persist to long distances, in contrast to surface patterns with  $q > q_0$  which persist only close to the surface. The  $q = q_0$  mode has both lengths  $\xi_q, \lambda_q$  diverging as  $(\chi_c - \chi)^{-1/4}$  for  $\chi \rightarrow \chi_c$ .

In Fig. 2 we give examples of the polymer morphologies in the case of three simple surface patterns. A uniform surface [in (a),  $\sigma = \sigma_0$  is constant] causes exponentially decaying density modulations to

propagate in the  $y$ -direction. A striped surface [in (b),  $\sigma = \sigma_q \cos(qx)$ ] creates a disturbance that is periodic in the  $x$ -direction, while decays exponentially in the  $y$ -direction. The combined surface pattern [in (c),  $\sigma = \sigma_0 + \sigma_q \cos(qx)$ ] induces density modulations which are the sum of the ones in (a) and (b).

A more complex chemical pattern, shown in Fig. 3(a), consists of V shaped stripes on the  $y = 0$  surface. The polymer density in parallel planes with increasing distance from the surface is shown in (b) and (c). Note how the frustration induced by the tips of surface chemical pattern [in (a)] is relieved as the distance from the surface increases. Surprisingly, similar morphology is observed when two grains of lamellar phase meet with a tilt angle, creating a tilt grain boundary in bulk systems [27].

Our treatment of confined BCP can be easily generalized to the case of two flat parallel surfaces [28]. The governing equation is still Eq. (5), but now there are four boundary conditions instead of the two in Eqs. (6) and (7). Figure 4 shows how two simple surface patterns

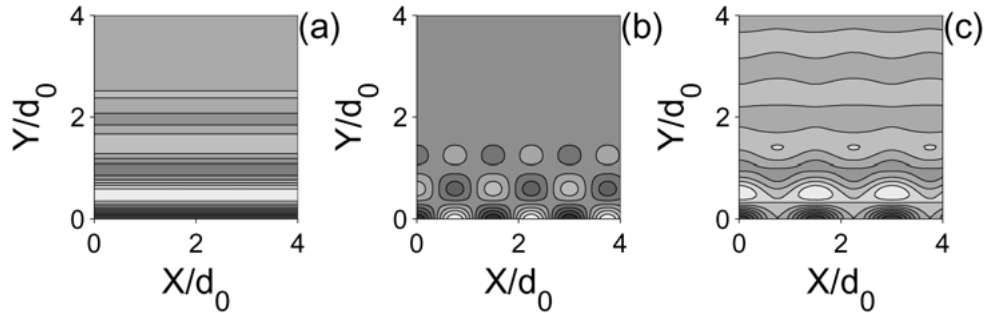


*Figure 2.* A BCP melt confined by one surface at  $y = 0$ . The B-monomer density is high in dark regions, while the A-monomer one is high in light regions. In (a) the surface is uniform,  $\sigma = 0.3$  and in (b) it has stripes given by  $\sigma = 0.3 \cos(\frac{2}{3}q_0x)$ . The “combined” effect is shown in part (c) where  $\sigma = 0.3 + 0.3 \cos(\frac{2}{3}q_0x)$  has a uniform and modulated part. The Flory parameter is  $N\chi = 10.2$ ,  $\tau_s = 0$  and lengths in the  $x$  and  $z$  directions are scaled by the lamellar period  $d_0$ .

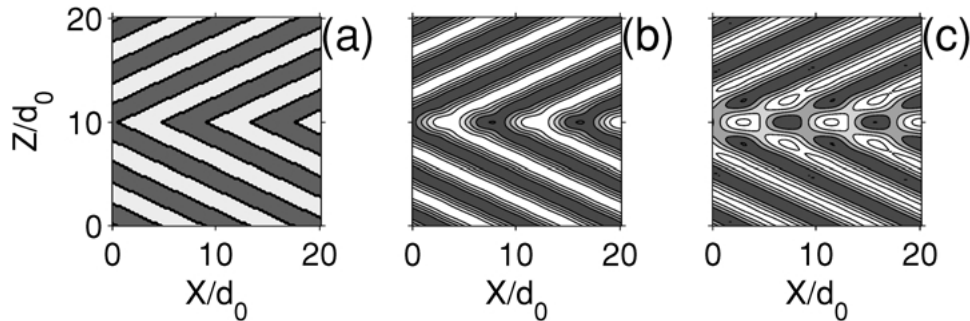


*Figure 3.* Propagation of surface pattern into the bulk. The surface pattern in the  $y = 0$  plane is shown in (a), where white (black) show regions preferring A (B) monomers. Parts (b) and (c) are contour plots of the polymer density at  $y = 3d_0$  and  $y = 8d_0$ , respectively.  $N\chi = 9.5$  and  $\tau_s = 0$ .

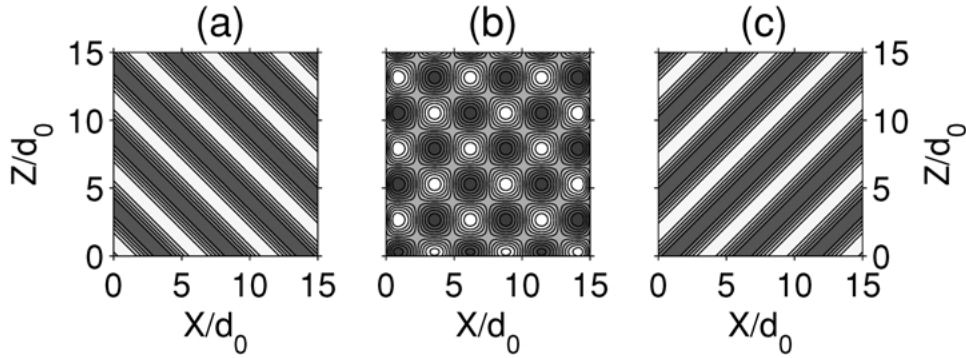


Figure 4. BCP melt confined by two flat parallel striped surfaces, depicted in parts (a) and (c), and located at  $y = -d_0$  and  $y = d_0$ , respectively. The melt morphology in the mid-plane ( $y = 0$ ) is shown in part (c). The Flory parameter is  $N\chi = 9$  and  $\tau_s = 0$ .

can be used to achieve a complex three-dimensional polymer morphology, even though the melt is in its bulk disordered phase. The stripes on the two surfaces are rotated by  $90^\circ$  with respect to each other. A symmetric “checkerboard” morphology appears in the mid-plane.

Up to this point, the BCP melt was assumed to be in its bulk disordered phase (above the bulk ODT point). When a melt in the lamellar phase (below ODT) is confined in a thin film, the morphology is dictated by a complex interplay between the natural periodicity and the imposed film thickness.

### 3. Confined Lamellar BCP

In this section we describe the ordering of lamellar BCPs confined by one or two surfaces. The phase behavior of thin BCP films in the lamellar phase subject to *uniform* surface fields has been investigated numerically using self-consistent field (SCF) theory [29, 30] and Monte-Carlo simulations [31, 32], and was found to consist of parallel, perpendicular and mixed lamellar phase denoted  $L_{\parallel}$ ,  $L_{\perp}$  and  $L_M$ , respectively. The latter  $L_M$  phase has parallel lamellae extending from one surface, which are then jointed in a T-junction defect with perpendicular lamellae extending from the opposite surface [33, 34]. At a given inter-surface spacing, increasing the (uniform) surface interactions promotes a parallel orientation with either A-type or B-type monomers adsorbed onto the surface. However, if the spacing  $L$  between the surfaces is incommensurate with the lamellar periodicity, or the incompatibility  $\chi$  is increased, a perpendicular orientation is favored [35–37].

In the treatment given below, a new effect can be observed when the surfaces are taken to be non-uniform, “striped”, with regions of alternating preferences to the

A and B blocks (see Fig. 1(c)). The stripe periodicity  $d_x$  is assumed to be larger than the natural (bulk) periodicity,  $d_x > d_0$ , and the stripes are modeled by

$$\sigma(x, z) = \sigma_q \cos(q_x x) \quad (10)$$

and are translational invariant in the  $z$ -direction. The surface  $q$ -mode is  $q_x = 2\pi/d_x < q_0$ .

Contrary to the system above the ODT, a linear response theory assuming small order parameter as a response to the surface field is inadequate here, since the bulk phase has an inherent spatially varying structure. Instead, we expand the order parameter around the bulk ordered phase.

$$\delta\phi(\mathbf{r}) \equiv \phi(\mathbf{r}) - \phi_b(\mathbf{r}) \quad (11)$$

where  $\phi_b$  is a “tilted” bulk lamellar phase given by

$$\phi_b = -\phi_L \cos(q_x x + q_y y) \quad (12)$$

$$q_x = q_0 \cos \theta, \quad q_y = q_0 \sin \theta, \quad (13)$$

The bulk ordering is depicted schematically as tilted lamellae in Fig. 1(c). For the correction order parameter  $\delta\phi$  we choose

$$\delta\phi(x, y) = g(y) \cos(q_x x). \quad (14)$$

This correction describes a lamellar ordering perpendicular to the surface, and commensurate with its periodicity  $d_x = 2\pi/q_x$ . The overall morphology of the lamellae is a superposition of the correction field  $\delta\phi$  with the tilted bulk phase, having a periodicity  $d_0$ . The region where the commensurate correction field  $\delta\phi$  is important is dictated by the amplitude function  $g(y)$ . The total free energy  $F = F_b + F_s$  is now expanded about its bulk value  $F[\phi_b]$  to second order in  $\delta\phi$ . The

variational principle with respect to  $g(y)$  yields a master equation:

$$[A + C \cos(2q_y y)]g(y) + Bg''(y) + g''''(y) = 0, \quad (15)$$

with parameters  $A$ ,  $B$  and  $C$  given by:

$$A = -\tau/h + q_y^4, \quad B = 2q_y^2, \quad C = -\tau/h. \quad (16)$$

This linear equation for  $g(y)$  is similar in form to Eq. (5) describing the density modulation of a BCP melt in the disordered phase. The lamellar phase is non-uniform and this results in a  $y$ -dependency of the term in square brackets. The above equation is readily solved using the proper boundary conditions (for more details see Refs. [26, 27]).

In Fig. 5 we present results for a BCP melt confined by one sinusoidally patterned surface,  $\sigma(x) = \sigma_q \cos(q_x x)$ , with no average preference to one of the blocks,  $\langle \sigma \rangle = 0$ , for several values of surface periodicity  $d_x$  and for fixed value of the Flory parameter  $\chi > \chi_c$ . The main effect of increasing the surface periodicity  $d_x$  with respect to  $d_0$  is to stabilize tilted lamellae, with increasing tilt angle. Note that even for  $d_x = d_0$  (Fig. 5(a)) yielding no tilt, the perpendicular lamellae have a different structure close to the surface as is induced by the surface pattern. Although the surface interactions are assumed to be strictly local, the connectivity of the chains causes surface-bound distortions to propagate into the bulk of the BCP melt. In particular, this is a strong effect in the weak-segregation regime we are considering.

So far in this section we have considered the semi-infinite problem of a BCP melt confined by one patterned surface. It is of experimental and theoretical

interest to study thin films of BCP when they are confined between a heterogeneous (patterned) surface and a second chemically homogeneous surface. This situation is encountered when a thin BCP is spread on a patterned surface. The second interface is the film/air interface and is homogeneous. Usually the free surface has a lower surface tension with one of the two blocks. This bias can be modeled by adding a constant  $\sigma_0$  term to the  $\sigma(x)$  surface field. For simplicity, we assume that the surface at  $y = -\frac{1}{2}L$  has purely sinusoidal stripes while at  $y = \frac{1}{2}L$  the surface is attractive to one of the A/B blocks with a constant preference:

$$\begin{aligned} \sigma(x) &= \sigma_q \cos(q_x x), & \text{at } y = -\frac{1}{2}L, \\ \sigma(x) &= \sigma_0, & \text{at } y = \frac{1}{2}L. \end{aligned} \quad (17)$$

A neutral surface at  $y = \frac{1}{2}L$  is obtained as a special case with  $\sigma_0 = 0$ . The expression (12) for the bulk tilted phase is modified ( $y \rightarrow y + \frac{1}{2}L$ ) in order to match the stripe surface pattern at  $y = -\frac{1}{2}L$ ,

$$\phi_b = -\phi_L \cos \left[ q_x x + q_y \left( y + \frac{1}{2}L \right) \right] \quad (18)$$

The homogeneous surface field at  $y = \frac{1}{2}L$  induces a lamellar layering parallel to the surface, since the two A/B blocks are covalently linked together. The simplest way to account for this layering effect is to include an  $x$ -independent term  $w(y)$  in our ansatz, Eq. (14), for the order parameter:

$$\delta\phi(x, y) = g(y) \cos(q_x x) + w(y). \quad (19)$$

The tilted lamellar phase confined by one homogeneous and one patterned surface is a generalization of

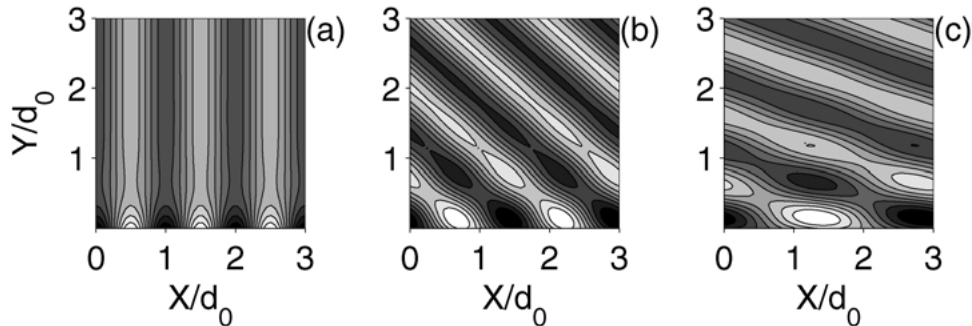


*Figure 5.* Tilted lamellar phase in contact with one patterned surface at  $y = 0$ . (See also Fig. 1(c)). The surface patterning is modelled by the term  $\sigma_q \cos(2\pi x/d_x)$ . The lamellae tilt angle  $\theta = \arccos(d_0/d_x)$  increases as the periodicity of the surface  $d_x$  increases:  $\theta = 0$  for  $d_x = d_0$  in (a),  $\theta \simeq 48.1^\circ$  for  $d_x = \frac{3}{2}d_0$  in (b) and  $\theta \simeq 70.5^\circ$  for  $d_x = 3d_0$  in (c). In the plots  $\sigma_q/hq_0^3\phi_L = 1$ . The Flory parameter  $N\chi = 11.5$  and  $\tau_s/hq_0^3 = 0.1$ .

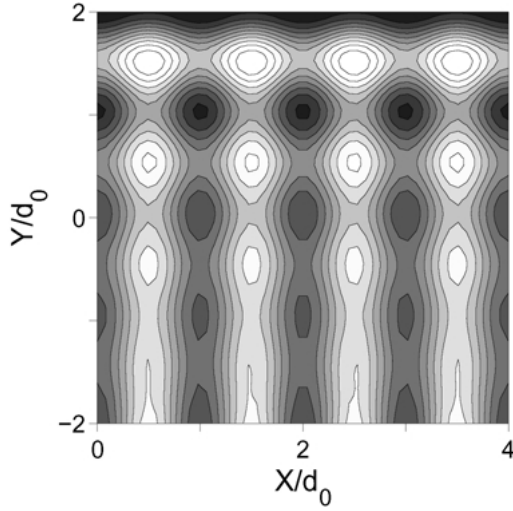


Figure 6. A BCP confined film showing a crossover from perpendicular lamellae at the  $y = -\frac{1}{2}L = -2d_0$  surface to parallel lamellae at the other surface,  $y = \frac{1}{2}L$ . The pattern on the bottom surface,  $\sigma(x) = \sigma_q \cos(q_0 x)$ , has the bulk periodicity  $d_0$ , and amplitude  $\sigma_q = 2hq_0^3$ , while the top surface ( $y = \frac{1}{2}L$ ) is homogeneously attractive to the B polymer (in black),  $\sigma_0 = 4hq_0^3$ . The Flory parameter is given by  $N\chi = 10.7$  and  $\tau_s/hq_0^3 = 0.4$ .

the mixed (perpendicular and parallel) lamellar phase, sometimes referred to as  $L_M$ . The latter morphology occurs when the surface imposed periodicity  $d_x$  is equal to the bulk periodicity  $d_0$ . This “T-junction” morphology, shown in Fig. 6, has perpendicular lamellae extending from the patterned surface. The homogeneous field at the opposite surface favors a parallel orientation of the lamellae. The crossover region between the two orientations is found in the middle of the film, and its morphology depends on temperature (the  $\chi$  parameter). The effect of the homogeneous field is evident, as parallel ordering extends from the top surface. We see here that strong enough modulated surface fields stabilize the tilted lamellar phases and, in particular, the  $L_M$  phase.

In the discussion above we have considered ordering mechanisms where the interaction of the polymers with the confining surfaces is mediated to regions far from the surfaces because of chain connectivity. We now turn to discuss orientation of BCP films in presence of external electric fields. This is a bulk ordering mechanism that does not originate from surface interactions.

#### 4. Alignment by Electric Fields

A well known mechanism to cause orientation or structural changes in polarized media is the “dielectric

mechanism”. This effect is based on the fact that when a material with inhomogeneous dielectric constant is placed in an electric field  $E$ , there is an electrostatic free energy penalty for having dielectric interfaces perpendicular to the field [8, 35, 36]. Thus, a state where  $\nabla\epsilon$  is perpendicular to the field  $\mathbf{E}$  is favored. For layered materials such as lamellar BCP phases, the strength of this effect is proportional to  $(\epsilon_A - \epsilon_B)^2 E^2$ , where  $\epsilon_A$  and  $\epsilon_B$  are the dielectric constants of the two micro-domains, and is enhanced when the difference in polarizabilities is large.

Let us first consider lamellae confined in a thin film with no electric field. We will then include an electric field and see its influence. For simplicity and brevity of presentation we assume that the Flory parameter  $\chi$  does not change on the surface,  $\tau_s = 0$ . We also concentrate on uniform surface fields with equal magnitudes,  $\sigma(y = -\frac{1}{2}L) = \pm\sigma$ ,  $\sigma(y = \frac{1}{2}L) = \pm\sigma$ . If the surface affinity  $\sigma$  is sufficiently large, the lamellae will order in a parallel arrangement as was discussed in the previous sections. These lamellae stretch or compress, increasing the bulk free energy, in order to decrease their surface energy. We mention below an adaptation [37] to the strong stretching approximation of Turner [38] and Walton et al. [39]. The lamellar period is  $d_0 = 2\pi/q_0$  and  $m$  is the closest integer to  $L/d_0$ . Depending on the value of  $\sigma$ , an integer ( $n = m$ ) or half integer ( $n = m + \frac{1}{2}$ ) number of lamellae fill the gap between the two surfaces. In the former case the ordering is symmetric (the same type of monomers adsorbed onto both surfaces), while in the latter it is asymmetric (A monomers adsorbed on one surface, whereas B monomers adsorbed on the other surface). The parallel lamellae are described by an order parameter  $\phi_{\parallel}$  given by [37]

$$\phi_{\parallel}(x, y) = \pm\phi_L \cos\left[q_{\parallel}\left(y + \frac{1}{2}L\right)\right] \quad (20)$$

The wavenumber is  $q_{\parallel} = 2\pi n/L$ , and the choice of  $\pm$  signs in Eq. (20) is such that the surface interactions, Eq. (2), are minimized. The perpendicular lamellae have the unperturbed bulk periodicity  $d_0 = 2\pi/q_0$  and their order parameter is simply given by

$$\phi_{\perp}(x, y) = \phi_L \cos(q_0 x) \quad (21)$$

We consider now the case where an electric field is turned on, in a direction that is perpendicular to the surfaces. Under conditions of constant voltage difference across the electrodes situated at the two bounding

surfaces, the minimum of the free energy is obtained by maximizing the capacitance. Since the A- and B-monomers have different dielectric constants, the effect of the electric field is to align the BCP layers parallel to the field, i.e. perpendicular to the surfaces. At a certain field strength this tendency starts to dominate over the preference induced by the surfaces to have parallel lamellae. Further increase of  $E$  above the threshold value gives rise to a perpendicular lamellar ordering.

In the weak segregation regime, the small value of density modulations  $\phi$  has been used [8, 11, 40] in order to write the electrostatic free energy as

$$\frac{Nb^3 F_{el}}{k_B T} = \beta \int (\hat{\mathbf{q}} \cdot \mathbf{E})^2 \phi_{\mathbf{q}} \phi_{-\mathbf{q}} d^3 q \quad (22)$$

$$\beta = \frac{(\varepsilon_A - \varepsilon_B)^2 Nb^3}{4(2\pi)^4 k_B T \langle \varepsilon \rangle} \quad (23)$$

Here  $\phi_{\mathbf{q}}$  is the Fourier transform of  $\phi(\mathbf{r})$ :  $\phi(\mathbf{r}) = \int \phi_{\mathbf{q}} \exp(i\mathbf{q} \cdot \mathbf{r}) d^3 q$ , and  $\hat{\mathbf{q}} = \mathbf{q}/q$  is a unit vector in the  $\mathbf{q}$ -direction. Copolymer modulations with a non-vanishing component of the wavenumber  $\mathbf{q}$  along the electric field, have a positive contribution to the free energy. In other words, there is a free energy penalty for having dielectric interfaces in a direction perpendicular to the electric field. In Eq. (23),  $\varepsilon_A$  and  $\varepsilon_B$  are the dielectric constants of the pure A and B-blocks, respectively [11], and  $\langle \varepsilon \rangle = \frac{1}{2}(\varepsilon_A + \varepsilon_B)$  is the average dielectric constant in the symmetric BCP film ( $f = \frac{1}{2}$ ). In the weak segregation regime, the spatial variations

in  $\phi$  are small and  $\varepsilon$  varies linearly with  $\phi$ ,

$$\begin{aligned} \varepsilon(\phi) &\simeq \left(\frac{1}{2} + \phi\right) \varepsilon_A + \left(\frac{1}{2} - \phi\right) \varepsilon_B \\ &= \langle \varepsilon \rangle + (\varepsilon_A - \varepsilon_B) \phi \end{aligned} \quad (24)$$

The total free energies of the parallel and perpendicular lamellae per unit area of the film are then given by

$$F_{\parallel} = \frac{1}{4} \left[ \tau + h(q_0^2 - q_{\parallel}^2)^2 + 2\beta E^2 + \frac{u}{16} \phi_L^2 \right] \phi_L^2 L + \Sigma \quad (25)$$

$$F_{\perp} = \frac{1}{4} \left[ \tau + \frac{u}{16} \phi_L^2 \right] \phi_L^2 L \quad (26)$$

$\Sigma = (\pm\phi_L \pm \phi_L)\sigma$  is the total surface interaction per unit area (Eq. (2)) at the two walls, and is negative. The  $\pm$  sign is determined from the  $\pm$  sign of the order parameter in (Eq. (20)). When the two surfaces are chemically identical, two similar signs in  $\Sigma$  mean symmetric ordering with an integer number of lamellae between the electrodes ( $\Sigma = \pm 2\phi_L \sigma$ ). In an antisymmetric ordering with a half-integer number of confined lamellae,  $\Sigma = 0$  as the two wall preferences cancel each other.

In Fig. 7 we compare the relative stability of parallel and perpendicular lamellae as a function of surface interaction strength  $\sigma$  (on the vertical axis) and surface separation  $L$  (on the horizontal axis). In (a) the electric field is zero. Parallel lamellae are favored when surface

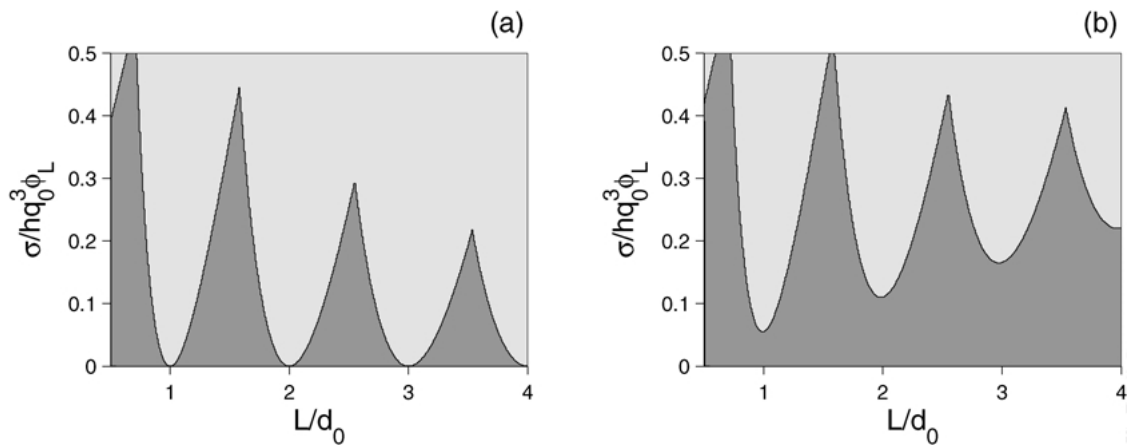


*Figure 7.* The stability of  $L_{\parallel}$  (in light) vs.  $L_{\perp}$  lamellae (dark), as a function of wall separation  $L$  and interfacial interaction parameter  $\sigma$ . The latter is taken as  $\sigma > 0$  on both surfaces. In (a) the electric field strength is zero, while in (b)  $E\sqrt{\beta} = 0.02$ . The  $L_{\parallel}$  phase is pushed upward in the stability diagram in (b), removing the degeneracy between  $L_{\perp}$  and  $L_{\parallel}$  that occurs for neutral walls ( $\sigma = 0$ ) for  $L/d_0$  being an integer number. The Flory parameter is  $\chi N = 11$ .

separation  $L$  is close to an integer value (recall that we take in this example two surfaces with the same polymer affinity  $\sigma$ ). Perpendicular ordering is favored when lamellae frustration is largest, i.e. when  $L/d_0$  is approximately a half-integer number. A degeneracy between the two states occurs for these values of  $L$  when the surface interactions vanish,  $\sigma = 0$ . For more details and a generalization to surfaces with different affinity for the A and B blocks see Ref. [37]. In (b) an electric field is applied in a direction perpendicular to the electrodes. As a consequence, perpendicular lamellae are favored and the boundary line between the light and dark regions in Fig. 7 is shifted upward to higher  $\sigma$  values.

In the strong segregation regime ( $\chi \gg \chi_c$ ), thin BCP films subjected to external electric field can be analyzed as well. Since in this regime the correlation length is not larger than the system size (in contrast to the weak segregation limit mentioned above), another *finite* length scale enters into the problem. The result is that the system has three possible states: parallel state in which

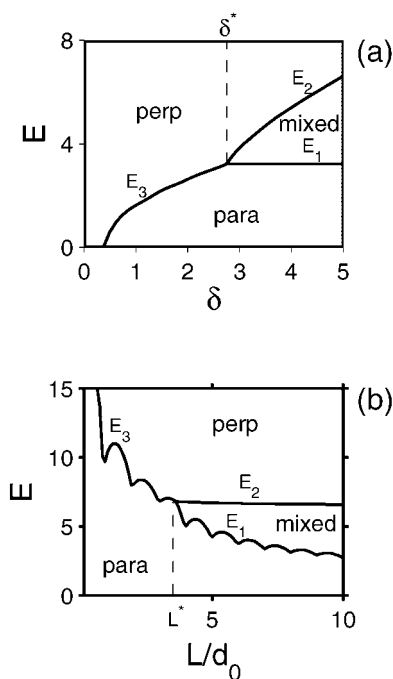


**Figure 8.** (a) Phase diagram in the  $E$ - $\delta$  plane.  $\delta$  is the difference between the A and B-block surface energies. When  $\delta < \delta^*$ , there is a direct transition between parallel and perpendicular lamellae at  $E = E_3$ . For  $\delta > \delta^*$ , a transition between parallel and mixed states occurs at  $E = E_1$ , followed by a second transition between mixed and perpendicular states when  $E = E_2 > E_1$ . (b) Similar diagram, but in the  $E$ - $L$  plane, where  $L$  is surface separation  $d_0$  is the lamellar period and  $\delta = 5$ .

parallel lamellae span the whole film, a perpendicular state, and a mixed state with parallel lamellae near the surfaces and perpendicular lamellae in the middle of the film. These three states are separated by three critical fields  $E_1$ ,  $E_2$  and  $E_3$ .

In Fig. 8(a) we show the phase diagram in the  $\delta$ - $E$  plane, where  $\delta$  is the dimensionless difference between then A and B-block surface energies and  $E$  is the strength of applied electric field. Transition from parallel to mixed lamellae at  $E = E_1$  occurs if  $\delta$  is above some threshold value,  $\delta^*$ . It is then followed by a transition between the mixed and perpendicular states at  $E = E_2$ . If  $\delta$  is small,  $\delta < \delta^*$ , there is a direct transition from parallel to perpendicular lamellae at  $E = E_3$ .

A different cut through the phase diagram in the  $L$ - $E$  (while keeping  $\delta$  constant) is shown in Fig. 8(b). A transition between parallel and mixed states occurs at  $E = E_1$ , followed by a second transition at  $E = E_2$  from the mixed to the perpendicular state, provided that surface separation is large enough,  $L > L^*$ . When  $L < L^*$  a direct transition between parallel and perpendicular lamellae occurs at  $E = E_3$ .

## 5. Summary

Several ordering mechanisms in confined BCPs are considered in this paper. Above the order-disorder temperature the polymer density near a chemically patterned surface is given as a function of the surface pattern. It is shown that each surface  $q$ -mode of the chemical pattern arises its own density mode, and that these modes can be regarded as uncoupled (linear response theory). The decay of these density modes into the bulk (away from the surfaces) is analyzed. In the weak segregation regime employed here, surface correlations become long range and hence simple chemical patterns (as in Fig. 4) can yield complex copolymer morphology, even though the bulk is in its disordered phase.

We describe lamellar BCP when they are confined by striped surface whose periodicity is larger than the lamellar periodicity. We find that in this case lamellae will tend to tilt with respect to the surface in order to optimize their surface interactions. The deviations from the perfect lamellar shape, induced by the surfaces, are obtained. These undulations of the lamellar interface are more prominent as the ODT is approached. Mixed lamellar phases appear when one surface has chemically patterns in the form of stripes while the other is uniform.

We examine the effect of an external electric field on the phase behavior of parallel and perpendicular lamellae. In the absence of any external electric field, we recover the previously obtained phase diagram [29–31]. The influence of electric field (Fig. 7(b)) is to favor the perpendicular lamellae: the region where parallel lamellae are stable is pushed up-wards in the phase diagram. We present as well the phase diagrams in the strong segregation regime. In this regime there are three possible system states (parallel, perpendicular and mixed) with three critical fields which separate them, as can be seen in Fig. 8(a) and (b).

The analytical calculations presented here together with other experimental and numerical studies are useful tools towards obtaining well controlled structures in the nanoscale. Indeed, the technical details employed should not obscure some simple results which are rather universal: the use of two simple one-dimensional striped surface patterns in order to achieve a complex three-dimensional morphology (Fig. 4), and surface field periodicity that facilitates control of tilt angle (Fig. 5). Finally, tuning the strength of electric field and surface separation (or interaction) as an external perturbation to create parallel, mixed or perpendicular lamellae (Fig. 8). These mechanisms call for further application-oriented studies as well as theoretical ones.

### Acknowledgments

Partial support from the U.S.-Israel Binational Foundation (B.S.F.) under grant No. 98-00429 and the Israel Science Foundation founded by the Israel Academy of Sciences and Humanities—centers of Excellence Program and under grant No. 210/02 is gratefully acknowledged. One of us (Y.T.) acknowledges support from the Chateaubriand Fellowship Program.

### References

1. I.W. Hamley, *The Physics of Block Copolymers* (Oxford University, Oxford, 1998).
2. Y. Cohen, R.J. Albalak, B.J. Dair, M.S. Capel, and E.L. Thomas, *Macromolecules* **33**, 6502 (2000).
3. Y. Cohen, M. Brinkmann, and E.L. Thomas, *J. Chem. Phys.* **114**, 984 (2001).
4. Z.-R. Chen, J.A. Kornfield, S.D. Smith, J.T. Grothaus, and M.M. Sattkowski, *Science* **277**, 1248 (1997).
5. Y.A. Vlasov, X.Z. Bo, J.C. Sturm, and D.J. Norris, *Nature* **414**, 289 (2001).
6. Y. Fink, J.N. Winn, S. Fan, C. Chen, J. Michel, J.D. Joannopoulos, and E.L. Thomas, *Science* **282**, 1679 (1998).
7. E. Schäeffer, T. Thurn-Albrecht, T.P. Russell, and U. Steiner, *Nature* **403**, 874 (2000).
8. Y. Tsori and D. Andelman, *Macromolecules* **35**, 5161 (2002).
9. G.G. Pereira and D.R.M. Williams, *Macromolecules* **32**, 8115 (1999).
10. B. Ashok, M. Muthukumar, and T.P. Russell, *J. Chem. Phys.* **115**, 1559 (2001).
11. K. Amundson, E. Helfand, X. Quan, and S.D. Hudson, *Macromolecules* **26**, 2698 (1993).
12. K. Amundson, E. Helfand, and X. Quan, *Macromolecules* **27**, 6559 (1994).
13. S. Walheim, E. Schäffer, J. Mlynek, and U. Steiner, *Science* **283**, 520 (1999).
14. T. Thurn-Albrecht, J. Schotter, G.A. Kästle, N. Emley, T. Shibauchi, L. Krusin-Elbaum, K. Guarini, C.T. Black, M.T. Tuominen, and T.P. Russell, *Science* **290**, 2126 (2000).
15. L. Leibler, *Macromolecules* **13**, 1602 (1980).
16. G.H. Fredrickson and E. Helfand, *J. Chem. Phys.* **87**, 697 (1987).
17. K. Ohta and K. Kawasaki, *Macromolecules* **19**, 2621 (1986).
18. Y. Tsori and D. Andelman, *Europhys. Lett.* **53**, 722 (2001).
19. J. Swift and P.C. Hohenberg, *Phys. Rev. A* **15**, 319 (1977).
20. M. Seul and D. Andelman, *Science* **267**, 476 (1995).
21. F.S. Bates and G.H. Fredrickson, *Annu. Rev. Phys. Chem.* **41**, 525 (1990).
22. S.A. Brazovskii, *Sov. Phys. JETP* **41**, 85 (1975).
23. G.J. Kellogg, D.G. Walton, A.M. Mayes, P. Lambooy, T.P. Russell, P.D. Gallagher, and S.K. Satija, *Phys. Rev. Lett.* **76**, 2503 (1996).
24. P. Mansky, T.P. Russell, C.J. Hawker, J. Mayes, D.C. Cook, and S.K. Satija, *Phys. Rev. Lett.* **79**, 237 (1997).
25. G.H. Fredrickson, *Macromolecules* **20**, 2535 (1987).
26. Y. Tsori and D. Andelman, *J. Chem. Phys.* **115**, 1970 (2001).
27. Y. Tsori, D. Andelman, and M. Schick, *Phys. Rev. E.* **61**, 2848 (2000).
28. Y. Tsori and D. Andelman, *Macromolecules* **34**, 2719 (2001).
29. M.W. Matsen, *J. Chem. Phys.* **106**, 7781 (1997).
30. G.T. Pickett and A.C. Balazs, *Macromolecules* **30**, 3097 (1997).
31. T. Geisinger, M. Mueller, and K. Binder, *J. Chem. Phys.* **111**, 5241 (1999).
32. Q. Wang, Q. Yan, P.F. Nealey, and J.J. de Pablo, *J. Chem. Phys.* **112**, 450 (2000).
33. G.G. Pereira and D.R.M. Williams, *Macromolecules* **32**, 1661 (1999); *Macromolecules* **32**, 758 (1999).
34. Q. Wang, S.K. Nath, M.D. Graham, P.F. Nealey, and J.J. de Pablo, *J. Chem. Phys.* **112**, 9996 (2000).
35. A. Onuki and J. Fukuda, *Macromolecules* **28**, 8788 (1995).
36. T. Thurn-Albrecht, J. DeRouchey, and T.P. Russell, *Macromolecules* **33**, 3250 (2000).
37. Y. Tsori and D. Andelman, *Eur. Phys. J. E* **5**, 605 (2001).
38. M.S. Turner, *Phys. Rev. Lett.* **69**, 1788 (1992).
39. D.G. Walton, G.J. Kellogg, A.M. Mayes, P. Lambooy, and T.P. Russell, *Macromolecules* **27**, 6225 (1994).
40. A.V. Kyrylyuk, A.V. Zvelindovsky, G.J.A. Sevink, and J.G.E.M. Fraaije, *Macromolecules* **35**, 1473 (2002).